ORIGINAL CONTRIBUTION

Manfred Wilhelm
Pierre Reinheimer
Martin Ortseifer

High sensitivity Fourier-transform rheology

M. Wilhelm (✉) · P. Reinheimer
M. Ortseifer
Max-Planck-Institut für Polymerforschung
Postfach 3148
D-55021 Mainz, Germany
e-mail:wilhelm@mpip-mainz.mpg.de

Abstract The application of oscillatory shear strain leads, in the non-linear regime, to the appearance of higher harmonic contributions in the shear stress response. These contributions can be analyzed as spectra in Fourier space with respect to their frequencies, amplitudes and phase angles. In this article, we present several theoretical and practical aspects of measuring Fourier rheology spectra with high sensitivity. Using the hardware of a conventional rheometer, Fourier rheology spectra with a signal-to-noise ratio of about 18,000:1 for a single acquisition were obtained. This allowed the observation of harmonics up to the 21st harmonic. Signal averaging can further increase the sensitivity.

Key words Fourier-transform rheology · Non-linear behavior · High sensitivity Fourier-transform rheology

Introduction

Non-linear effects become increasingly important when the shear rate exceeds the inverse of the longest relaxation time of the system under investigation (Malkin 1995). A measure of non-linear conditions is given by the product of the relaxation time τ and the shear rate $\dot{\gamma}$, which is referred to as the Deborah number $D = \tau\dot{\gamma}$. The description and understanding of non-linear behavior is important because it is frequently encountered during the processing of materials in general and of polymers in particular (Macosko 1994). The application of an oscillatory shear strain with a single frequency ω_1 results, for non-Newtonian materials, in the generation of odd higher harmonic contributions at $(2n + 1)\omega_1$ within the shear stress response (Giacomin and Dealy 1993; Wilhelm et al. 1998).

Using the Fourier approach, these different harmonics in the shear stress response can be analyzed with high precision. In the literature, this concept has been applied to the linear regime (Öttinger and Zylka 1992; Holly et al. 1988) and also to the non-linear regime (Gamota et al. 1993; Giacomin and Dealy 1993; Reimers and Dealy 1996, 1998). In this article we would like to extend the current state-of-the-art sensitivity for this type of analysis by several orders of magnitude. Both the experimental and theoretical aspects of Fourier transformation (FT) are covered.

The basic mathematics that leads to the appearance of higher harmonics in the stress response has already been described, for example in Wilhelm et al. (1998). Therefore only a very brief summarization of the arguments is recited.

Consider the non-Newtonian case where the viscosity related shear stress is no longer proportional to the shear rate. In this case the non-Newtonian viscosity η can be expanded as a function of the absolute shear rate. This is done under the assumption that the shear strain, and consequently the shear rate, are purely sinusoidal functions. The non-Newtonian behavior leads then to the generation of higher harmonic contributions in the resulting shear stress. The result for the time dependent shear stress τ is finally given by:

$$\tau(t) = A\cos\omega_1 t + B\cos 3\omega_1 t + C\cos 5\omega_1 t + \ldots.$$

or equivalently

$$\tau(t) = \sum_{n,\text{odd}} a_n \cos(n\omega_1 t + \phi_n) \ . \tag{1}$$

The prefactors A, B and C are in general complex numbers, whereas the a_n values refer to the absolute intensity of each harmonic. An FT can unravel the frequencies $n\omega_1$, amplitudes a_n, and phase angles ϕ_n of all contributions within the shear stress response, as described in Eq. (1). For details regarding the mathematical aspects of FT see, for example, the textbooks by Ramirez (1985) or Bracewell (1986).

Fourier-related considerations

To achieve FT-rheology spectra with a high sensitivity, a half-sided, discreet, complex, magnitude FT was applied to the shear stress signal. To obtain highly resolved, artifact-free spectra with a low noise level, the time signal must be acquired carefully, taking several mathematical and experimental aspects of the FT into account. A specific summary of the most important aspects is given below, although this is textbook knowledge. A more extended discussion of FT can be found in the following references: Ramirez (1985), Bracewell (1986), Ernst and Anderson (1966), Schmidt-Rohr and Spiess (1994).

The FT of any real or complex time signal $s(t)$ or frequency-dependent spectrum $S(\omega)$ is usually defined in the following way:

$$S(\omega) = \int_{-\infty}^{\infty} s(t) e^{-i\omega t} \, dt$$

and

$$s(t) = \frac{1}{2\pi} \int_{-\infty}^{\infty} S(\omega) e^{+i\omega t} \, d\omega \quad . \tag{2}$$

The prefactors in Eq. (2) may differ depending on the conventions used. The FT in general is an invertible, complex transformation over the infinite integral from $-\infty$ to $+\infty$. The FT arranges the time-dependent signal $s(t)$ with respect to the different frequencies $S(\omega)$ present within the time domain.

An important mathematical property of the FT is linearity:

$$s(t) + g(t) \xrightarrow{\text{FT}} S(\omega) + G(\omega) \quad . \tag{3}$$

This means that any superposition of different frequencies in the time domain will also be resolved in the frequency domain. The FT is inherently complex; thus even for a real time-domain data set $s(t)$, this transformation results in a complex spectrum $S(\omega)$ with a real $r(\omega)$ and imaginary part $i(\omega)$. Alternatively, the complex spectra can be presented as magnitude $m(\omega)$ and phase $\phi(\omega)$ spectra, respectively, where $\tan \phi = i/r$ and $m = (r^2 + i^2)^{1/2}$. By applying the Euler relation $(\exp(i\phi) = \cos\phi + i\sin\phi)$, the basic definition in Eq. (2) can be separated into a cosine and sine transformation, simply termed a Fourier cosine and Fourier sine transformation.

A half-sided FT is obtained when the integration in Eq. (2) uses only half the integral limits, specifically from $t = 0$ to $t = +\infty$. In this case the FT is similar to a complex Laplace transformation. A half-sided FT is the most common one used for experimental data.

In the case of discrete and digitized sampling, the data is taken point by point with a fixed increment t_{dw} (dwell time, or inverse sampling rate) over a total time $t_{aq} = t_{dw}N$ (acquisition time). From N real (or complex) data points in time, by means of a discrete FT, a discrete spectrum of N complex points is generated. The spectral width is the maximum detectable frequency, and is given by the sampling rate $\omega_{max}/2\pi = \nu_{max} = 1/(2t_{dw})$. The spectral width is also sometimes called the Nyquist frequency. The frequency difference between two points of the spectrum is given by $\Delta\nu = 1/t_{aq}$, and is termed the spectral resolution. In any experiment one should first estimate the maximum possible harmonic contribution and adjust the sampling rate accordingly. For example, a shear frequency of 1 Hz and an investigation up to the 25th harmonic at 25 Hz leads to a minimum sampling rate of 50 1/s ($t_{dw} = 20$ ms) or, to be on the safe side experimentally, $t_{dw} \approx 10$ ms. Due to the fact that the peaks in the FT-rheology spectrum are in principle extremely narrow, a long acquisition time t_{aq} decreases the observed line width and increases the signal-to-noise (S/N) ratio. The S/N ratio can be defined as the ratio of the amplitude for the highest peak ("signal") divided by the standard deviation of the noise ("noise"). The noise level should be measured in a spectral window where no peak is anticipated. Typically, we acquired about 20–50 cycles of the fundamental frequency for each sweep. This leads to a number of acquired time data points N in the range 2000–5000. Optimum conditions do not seem to be met in specific cases in the published literature.

Longer acquisition times increase the S/N ratio. To explain this fundamental statement, we use Eq. (2) and first compare the integral over the spectrum $S(\omega)$ with the time data $s(t)$ at $t = 0$:

$$s(0) = \frac{1}{2\pi} \int_{-\infty}^{\infty} S(\omega) \underbrace{e^{+i\omega 0}}_{1} \, d\omega = \frac{1}{2\pi} \int_{-\infty}^{\infty} S(\omega) d\omega \quad . \tag{4}$$

In Eq. (4) the value for the time-dependent signal $s(t)$ at $t = 0$ does not change as a function of the acquisition time t_{aq} and, consequently, the integral over the spectrum cannot change either. Increasing t_{aq} decreases the observed line width or equivalently increases the spectral resolution, $\Delta\nu$, as already described. Thus this leads to an increased S/N ratio. Further increases in the S/N ratio can be achieved by applying apodization functions. Spectral resolution can be improved using zero filling. Neither of these two topics is of primary importance in the case of a forced oscillation under

steady state because the forced oscillation itself lasts ideally forever. Interested readers are referred to the specific literature in Ramirez (1985), Bracewell (1986) or Schmidt-Rohr and Spiess (1994).

In most experiments the time data $s(t)$ is not measured continuously but discretely, after fixed time steps, and it is digitized subsequently. Analog time data is digitized every dwell time t_{dw}. This procedure is done via a k bit analog-to-digital converter (ADC). A k bit ADC has $2^k - 1$ discrete values to discriminate a single point in time. Double-precision arithmetic increases this by a factor of two. In practice we recommend values of $k \geq 8$. Higher values of k lower the minimum detectable intensity for weak signals (Skoog and Leary 1992; Homans 1989). A low bit ADC can be a limiting factor for measurements where a very high S/N ratio is desired.

The important concepts of dwell time, acquisition time, spectral width and spectral resolution are visualized in Fig. 1. In this figure 1000 time data points for 25 oscillations have been calculated prior to a Fast Fo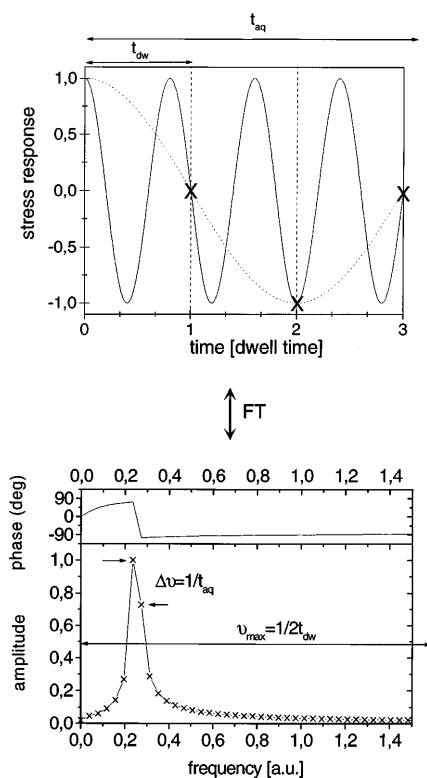urier transformation (FFT). An FFT is a very common and particularly fast algorithm for discrete FT in which the calculation time rises only as $N\log_2 N$, instead of increasing as N^2 as in a brute force discrete FT approach. While the general discrete FT is formulated for arbitrary numbers of points N, the simplest and most common FFT ("butterfly") algorithms require $N = 2^n$ (Cooley and Tuckey 1965; Higgins 1976). This restriction leads to fixed values for the acquisition time t_{aq} and thus also for the spectral resolution $\Delta v = 1/t_{aq}$. As a result, the fundamental frequency $\omega_1/2\pi$ and the odd multiples $n\omega_1/2\pi$ are often not exactly at specific spectral points. The application of an FFT can therefore introduce misleading results for the intensities and phases of the spectral intensities, because they cannot be read at exactly the expected frequency value. The experimental data within this article were consequently not processed using the common butterfly FFT algorithm.

FT-rheology also allows data averaging of spectra. Spectral averaging, in general, increases the S/N ratio of the acquired data proportional to the square root of the transients n, i.e., $S/N \propto \sqrt{n}$. This allows, at least in principle, an unlimited S/N ratio. In contrast to FT-infrared or FT-nuclear magnetic resonance spectroscopy, the rheology response does not have the same phase for different harmonics ($\phi_n \neq \phi_m$). Still, the relative phases for each harmonic are reproducible with respect to the phase of the applied oscillatory strain.

To overcome the sensitivity problem partially, averaged FT-rheology spectra can be acquired by computing a magnitude mode spectrum directly after each single measurement ("sweep") and afterwards adding the spectra successively. This method loses the phase angle information, but measures the relative intensities between the different harmonic contributions with increasing precision. To avoid the loss of the phase angle information, the data acquisition should be triggered with respect to the harmonic excitation. In this case intensity and phase information are preserved. An example of data averaging is also presented in the results section.

Experimental

Data were obtained using a Rheometrics Dynamic Analyzer RDA II rheometer and a Rheometrics RFS II rheometer. The raw stress data were analyzed as obtained from the rheometer. The discrete FT was done using a LeCroy Oscilloscope 9304 C with the appropriate FT package incorporated. Additionally, FFT analysis was applied using the programs Origin 4.1 and 5 (Microcal Software). A cone-plate geometry was used with a diameter of 50 mm and a 0.02 rad cone angle. The sample under investigation was a 10% solution of polyisobutylene ($-C(CH_3)_2-CH_2-)_n$ with molecular weights of $M_v = 1.11 \cdot 10^6$ and $4.6 \cdot 10^6$ g/mol. The bulk entanglement length of this polymer is 8900 g/mol according to Ferry (1980). The polymer was dissolved in 90% oligoisobutylene. The oligoisobutylene had a molecular weight of about 120 g/mol as

Fig. 1 Basic scheme of a discrete Fourier transformation (FT). The time-dependent signal is analyzed with respect to the different frequency components. Due to the discrete signal a minimum time increment, the so-called dwell time (t_{dw}), leads to ambiguities with respect to different frequencies. This phenomenon results in a specific spectral width (the maximum unambiguous detectable frequency). The maximum data acquisition time (t_{aq}) limits the minimum resolution of the spectrum

determined by gel permeation chromatography and mass spectrometry. ^{1}H nuclear magnetic resonance spectroscopy on the solvent determined a small amount ($< 5\%$) of olefinic protons, while the rest of the molecule was completely aliphatic. The trade names of the two samples are Oppanol B 100 ($1.11 \cdot 10^6$ g/mol) and Oppanol B 200 ($4.6 \cdot 10^6$ g/mol). Both are produced and distributed via BASF.

To reduce the mechanical noise level, the rheometer was kept in a rigid and mechanically stable environment. For all electronic connections, double-shielded BNC-type cables (e.g., RG 223) were used to minimize the electronic noise level. The raw data from the force transducer were checked to ensure that they were quantitative. This was verified by comparing the FT results for the phase angle δ of the fundamental response in the linear regime with the built-in data analysis of the rheometer. The values for the phase angle were similar to within $\pm 0.2°$. The possibility of phase shifts due simply to the rheometer hardware can consequently be excluded.

Results and discussion

In this section experimental results illustrate different aspects of the previous discussion. The experimental results cover the following topics: first, typical rheology data in both time and frequency domains are presented. The intensity $I(\omega)$ and phase of these types of measurements are shown as a function of increasing shear strain. Furthermore, the reproducibility and precision of these measurements are established. The parallel plate and the cone-plate geometry are compared using the non-linear regime. Also, examples are shown where spectral averaging leads to a significant enhancement in sensitivity. Finally, the Fourier approach is applied to determine the linear/non-linear crossover in a polyisobutylene sample. Polyisobutylene was used because of its simplicity as a fully amorphous high molecular weight homopolymer.

Figure 2 displays a typical stress response for an oscillatory shear strain experiment at 0.1 Hz using Oppanol B 200. In this experiment the polymer solution was sheared with a sinusoidal strain of 2400% amplitude. The time-dependent stress response is displayed in Fig. 2a. From the time data, it is already clear that in addition to a single sinusoid, higher harmonic contributions are present in the shear stress response. The FT of the data in Fig. 2a is displayed in Fig. 2b. In accordance with Eq. (1), only the odd higher multiples of the fundamental frequency are detected. The inset of Fig. 2b is magnified by a factor of 100. The inset visualizes the high S/N ratio reached for a single sweep. This specific measurement achieved an S/N ratio of 17 008:1 as calculated with respect to the stress response at 0.1 Hz. The 21st harmonic is the highest harmonic with a significant contribution above the noise level.

A simplified model of the time-dependent response function under extreme shear thinning is given by a periodic step function for the shear stress (Wilhelm et al.
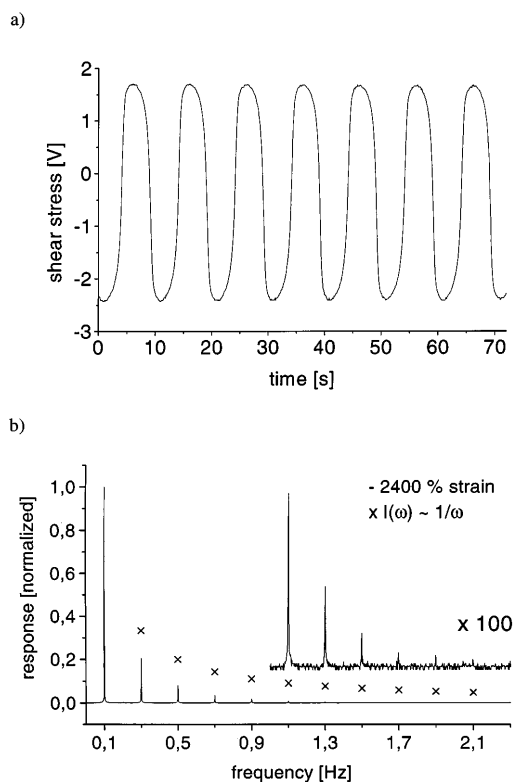

Fig. 2 **a** Experimental time data for the stress response after applying a sinusoidal strain at 0.1 Hz and 2400% amplitude to a polyisobutylene sample. For simplicity, only part of the time data is shown. The sample was Oppanol B 200 ($M_v = 4.6 \cdot 10^6$ g/mol) dissolved in 90% oligoisobutylene solution, measurements were made at 353 K. **b** The magnitude FT spectrum resolves the contributions of the higher harmonics up to the 21st overtone at 2.1 Hz. The *inset* displays the spectrum of a single sweep magnified 100 times. The S/N ratio for this spectrum is 17,008:1. The *crosses* in the spectrum symbolize the intensity expected for different harmonics as a result of a simplified step model

1998). A periodic step function has only odd Fourier components at ω_1, $3\omega_1$, $5\omega_1$, etc. For this function, the different intensities $I(n\omega_1)$ along the frequency axis are proportional to $I(n\omega_1) \propto 1/n$, so normalized to the fundamental frequency we expect: $I(\omega_1) = 1$, $I(3\omega_1) = 1/3$, $I(5\omega_1) = 1/5$, etc. The experimental Fourier analysis of the spectrum in Fig. 2b allows the observation of harmonics up to $I(21\omega_1)$. The crosses in Fig. 2b display the expected intensity resulting from the simplified model. Clearly the experimental data decay much faster. One difference between the simple step function model and the experimental data is the absence of sharp edges in the time domain of the experimental data. As a consequence, the intensity of the odd harmonics is not expected to follow the indicated $I(n\omega_1) \propto 1/n$ approximation closely but rather to decay faster. This is also due to the memory terms involved. The value of the relative intensities at different frequencies consequently reflects the degree of non-linearity and also the memory-related

behavior. Any folding of a memory function in the time domain results in a simpler multiplication in the frequency domain (Reinheimer et al. 1999).

To evaluate the accuracy and reproducibility of FT-rheology spectra with respect to the experimental conditions, we measured different Oppanol B 200 samples, on 5 different days. In these experiments, an oscillatory strain with 0.1 Hz and 1900% shear strain was applied. The results of the intensity of the third harmonic $I(3\omega_1)$ with respect to the fundamental frequency $I(\omega_1)$, and the related phase shift between the pure sinusoidal shear strain and the stress response, are given in Table 1. The reproducibility of the relative intensities at $I(3\omega_1)/I(\omega_1)$ is within 0.2%. Furthermore, the relative phase of the third harmonic is accurate to within $\pm 0.7°$. One should be aware that the relative phase of the oscillation for the nth harmonic relative to the applied phase of the strain oscillation can only be defined within the interval $\phi_n \in [-180°/n; +180°/n]$. The relative phase of each harmonic overtone has a time period $T_n = 2\pi/(\omega_1 n)$ for the nth overtone. As a comparison the phase angle δ in the linear regime at 0.1 Hz was 22.9°, the phase angle δ at 1900% shear strain amplitude and 0.1 Hz was measured to be 77.6° and the phase angle δ in the linear regime for an excitation with 0.3 Hz was measured to be 9.8°. To obtain absolute values for each phase with respect to the shear excitation, the different period for each harmonic contribution must be scaled accordingly.

Figure 3 shows five typical spectra at 353 K for Oppanol B 200, as a function of increasing strain. Values for the strain amplitude in these spectra are 5, 58.3, 400, 1400 and finally 2400%. In each case a 0.1-Hz oscillation was applied. For the amplitude value of 2400%, the related spectrum is also already shown in Fig. 2b. Increasing the strain generates an increasing number of higher harmonic contributions due to the increasing non-linearities involved. One way to characterize the degree of non-linearity is the intensity ratio of the third harmonic $I(3\omega_1)$ relative to the fundamental frequency

$I(\omega_1)$. Measurements from these spectra can provide a crucial test regarding analytical or numerical model predictions with respect to the non-linear response regime (Rouault and Kremer 1999).

In the following step we evaluated the influence of different shear geometries. The cone-plate geometry has the advantage of a constant shear rate across the sample. In the linear response regime the cone-plate geometry is often replaced by the parallel plate geometry. The parallel plate case benefits from even simpler geometry and the possibility of applying very large shear strains at small gaps between the two plates. In the linear regime the difference between the two geometries can be compensated for by an appropriate shift factor (Macosko 1994), where the characteristic radius r of the parallel plate geometry with respect to the total radius R of the plates is $r/R = 0.75$. The characteristic radius of the parallel plate geometry mimics the position where the shear rate in the linear regime is similar to the shear rate of the cone-plate geometry. To compare parallel plate and cone-plate geometry in the non-linear regime, Oppanol B 100 at 0.1 Hz was measured as a function of increasing strain. The degree of non-linear behavior was characterized via the ratio of intensities $I(3\omega_1)/I(\omega_1)$. The results for these measurements are shown in Fig. 4a. The application of a shift factor of 0.75, as used in the linear regime, clearly improves the relative discrepancy between the two geometries (see Fig. 4b). The two data sets still do not have exactly the same dependency. The experimental values differ at large strains but for lower strains they display similar values and also a similar slope. This leads to the conclusion that the application of a single shift value in the non-linear regime is in principle difficult. This is caused by the spatial inhomogeneous shear rate and therefore inhomogeneous shear response along the parallel plate geometry. Consequently, different geometries cannot be compensated for by a single characteristic radius at different strain amplitudes within the non-linear regime.

A further option using FT-rheology has been mentioned earlier, namely, averaging n shear stress spectra and therefore increasing the S/N ratio. In theory the increase should be: $S/N \propto \sqrt{n}$. Figure 5 displays the effect of signal averaging on an Oppanol B 100 sample where a 1-Hz oscillation with 400% shear strain was applied. In Fig. 5a, a section of the normalized $(I(\omega_1) = 1)$ shear stress spectrum is displayed for the case of a single sweep. Clearly, the 5th harmonic at $5\omega_1$ is visible, while the peak at $7\omega_1$ is within the noise level. After averaging 100 independent sweeps, the sensitivity or the S/N ratio has increased by the predicted factor of 10 (see Fig. 5b). It is possible to detect the intensity for the harmonic contribution at $7\omega_1$ and even the contribution at $9\omega_1$ is visible. The calculated values for the the S/N ratio are 4515:1 in Fig. 5a and 44 889:1 in Fig. 5b. This is in good agreement with the theoretically expected

Table 1 Average values for $I(3\omega_1)/I(\omega_1)$ as received from 5 independent measurements of the relative intensity and relative phase of the contribution at $3\omega_1$. A strain of 1900% amplitude and 0.1 Hz frequency was applied a Oppanol B 200 solution at room temperature. The displayed values show the high reproducibility for this characterization method

Experiment	$I(3\omega_1)/I(\omega_1)$	Phase angle ϕ_3
1	0.1677	41.97°
2	0.1660	41.92°
3	0.1694	43.36°
4	0.1674	42.17°
5	0.1711	43.16°
Average	0.16830	42.52°
Standard deviation	0.002	0.69°

Fig. 3a–e FT-rheology stress spectra as a function of the shear strain amplitude. The applied strain amplitude varied from 5, 58.3, 400, 1400 to 2400%. Measurements were performed at 353 K using an Oppanol B 200 solution and applying a 0.1-Hz oscillation. Increasing the shear strain amplitude enlarges the degree of non-linearity. This is directly reflected in the generation of more and more pronounced overtones. For each spectrum only a single sweep was acquired. The measured S/N ratio is indicated for each spectrum
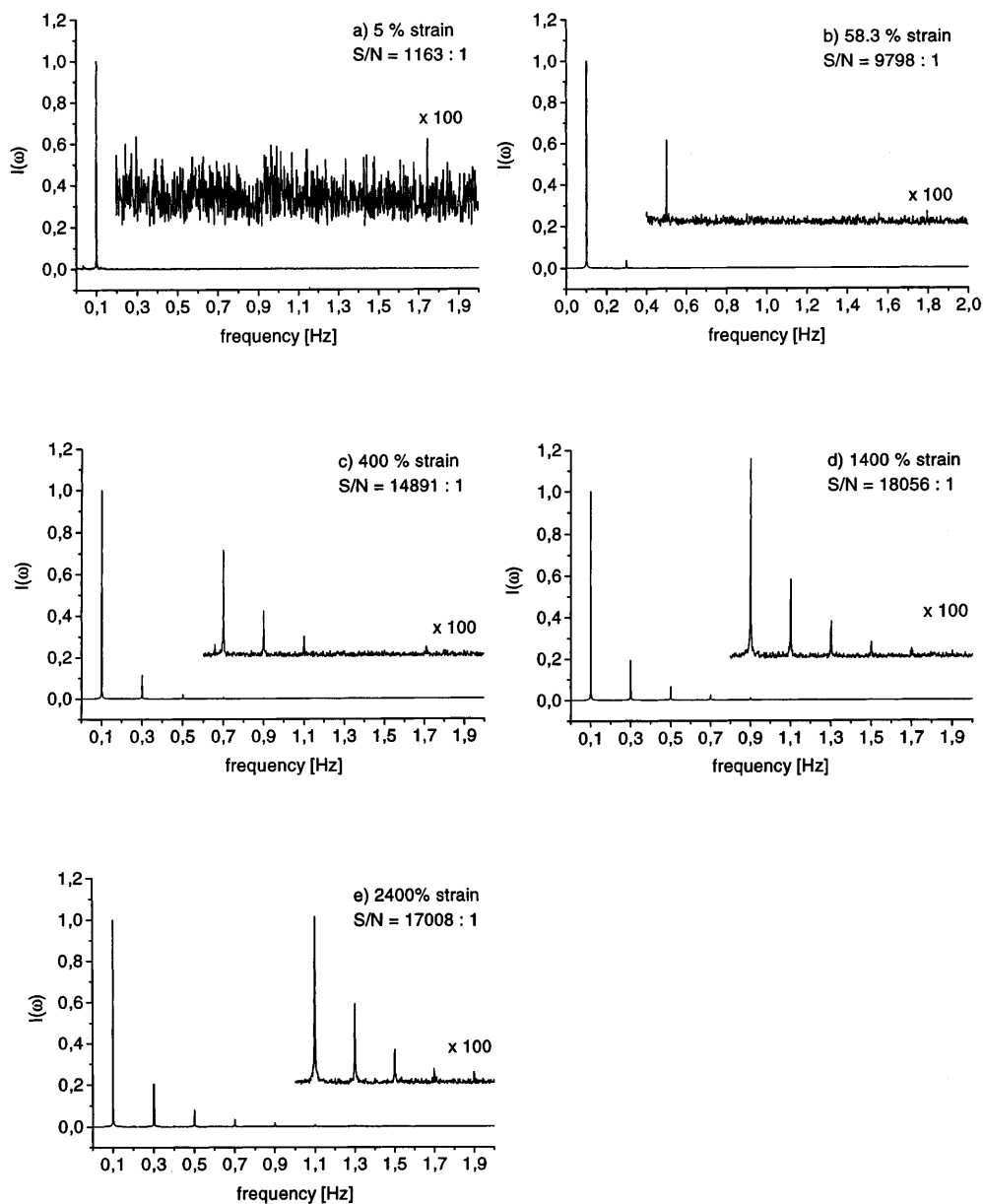
increase by a factor of 10. Averaging magnitude spectra gives increased sensitivity with respect to the amplitude of the harmonics. This allows the determination of a_n in Eq. (1) with great accuracy. The technique of averaging magnitude spectra does not allow the detection of the phase angle ϕ_n for each of the harmonics. Although the measurement of the phase angle ϕ_n is in principle also feasible if the phase of the applied strain is used to trigger the data acquisition. This way the spectra can always be added with a similar response phase.

So far we have demonstrated that FT-rheology stress spectra can be measured with very high sensitivity. This technique now offers a wide range of possibilities and practical applications. Applications include from the pure description of non-linear material, including the reconstruction of the time data. The comparison of theoretical (Bird and Carreau 1968; De Gennes 1979; Doi 1996; Ferry 1980; Larson 1988) and computer models with the experimental data of polymers or other materials is another possibility. Also, the kinetics of time-dependent phenomena, for example, shear-induced phase separation, can be studied.

In Fig. 6, we plot the increasing amplitude for the third harmonic as a function of shear strain amplitude where a sinusoidal oscillation with 0.1 Hz was applied (at 293 K) to Oppanol B 100. The maximum shear rate during a cycle can be calculated as: $\dot{\gamma}_{\max} = \gamma_0 \omega = \gamma_0 2\pi\nu$, where γ_0 is the strain amplitude. The increase in $I(3\omega_1)/$
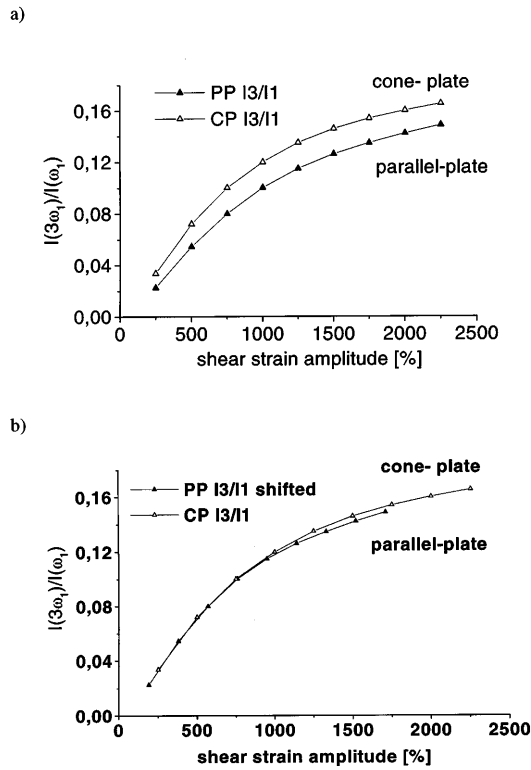
a)

b)

Fig. 4 a Comparison of the non-linear response using plate-plate and plate-cone geometry. The ratio $I(3\omega_1)/I(\omega_1)$ was used to characterize the non-linear response. This ratio was measured as a function of the shear strain amplitude at 0.1-Hz excitation. **b** The application of a shift factor of 0.75 clearly reduces the discrepancies between the two geometries. The application of the shift factor does not result in absolutely identical data and therefore the results depend on the geometry in the strongly non-linear regime
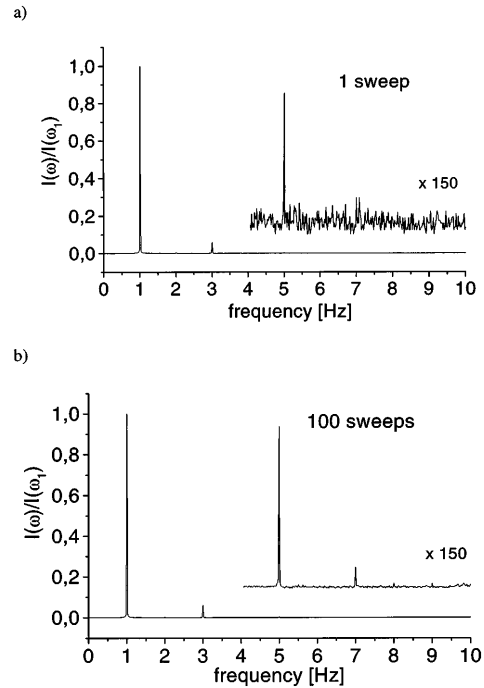
a)

b)

Fig. 5 Application of a 1-Hz sinusoidal excitation with 400% shear strain amplitude using a Oppanol B 100 solution. In both cases we show a normalized ($I(\omega_1) = 1$) magnitude spectrum. In **a** the spectrum after only a single sweep is displayed. Clearly, the 5th harmonic at 5 Hz is visible while the peak at 7 Hz is not clearly resolved and is within the noise level of the single measurement. Averaging 100 sweeps as shown in **b** theoretically increases the signal-to-noise (S/N) ratio by a factor of $100^{0.5} = 10$. This enables the peak at 7 Hz to be resolved and even the peak at 9 Hz is detectable. The averaging technique allows, in principle, an unlimited S/N ratio. In **a** we calculated an S/N ratio of 4515:1, whereas in **b** we calculated 44,889:1
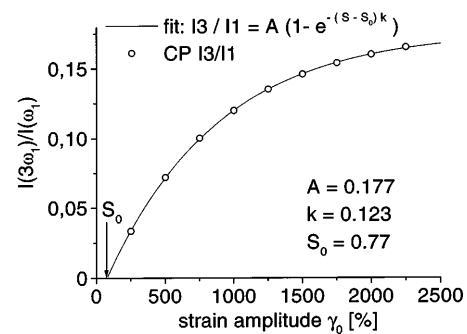
$I(\omega_1)$ as a function of strain can be described by an exponential function (Reinheimer et al. 1998) where the intercept for $I(3\omega_1)/I(\omega_1) = 0$ defines the crossover from linear to non-linear behavior. In the case of Oppanol B 100, we also determined the parameter for steady shear according to the Carreau model (Bird and Carreau 1968) where $\eta/\eta_0 = 1/(1 + (\beta|\dot{\gamma}|)^{\alpha})$ is assumed. In this model the parameter β determines the crossover between linear and non-linear behavior. The parameters according to the Carreau model were measured (not shown) as $\eta_0 = 172$ Pa s, $\beta = 0.62$ s and $\alpha = 0.82$. The exponential analysis for the third harmonic as a function of strain leads to a crossover amplitude $S_o = 77\%$. This is the amplitude where the onset of non-linear behavior occurs and the maximum shear rate $\dot{\gamma}_{max}$ within a cycle exceeds the inverse of the longest relaxation time. For the value of $S_o = 0.77$ shear strain amplitude we find a crossover shear rate of $\dot{\gamma}_{max} = 0.77 \times 2\pi \times 0.1[1/s] = 0.48[1/s]$. This value should be the inverse of the longest relaxation time in the polymer solution.

Fig. 6 Increases in the intensity of $I(3\omega_1)/I(\omega_1)$ as a function of the applied shear strain amplitude using a cone-plate geometry. The shear frequency was 0.1 Hz for an Oppanol B 100 solution. The increase in the third harmonic can be described over a wide range with a single exponential function. The onset of contributions at $I(3\omega_1)$ determines the crossover from linear to non-linear behavior. We found the onset at a shear strain amplitude of $S_0 = 0.77$. For this strain value the maximum shear rate reaches up to 0.48 s^{-1} during a shear cycle

The experimental analysis (Reinheimer et al. 1998), the analysis using the Carreau model and also computer simulations (Rouault and Kremer 1999) with respect to $I(3\omega_1)/I(\omega_1)$ could in all cases be fitted by a single exponential increase as a function of shear strain. In the case of samples where the linear regime is experimentally inaccessible, the hypothetical crossover from linear to non-linear shear behavior might be found by extrapolating back to lower shear rates.

Conclusion

In this article, we describe several fundamental considerations for measuring higher harmonics in the shear stress response. Fundamental principles of FT rheology and the consequences for practical data acquistion are discussed. We are able to observe up to the 21st overtone with an overall S/N ratio of about 15,000:1 for a single sweep. The impact of parallel plate and cone-plate geometry is analyzed and also different possibilities for further increasing the sensitivity of these measurements are stated. Practical applications are discussed and the crossover from linear to non-linear behavior is analyzed in a specific case.

References

Bird RB, Carreau PJ (1968) Chem Eng Sci 23:427

Bracewell RN (1986) The Fourier transform and its application. McGraw-Hill, New york

Cooley JW, Tuckey JW (1965) Machine calculation of complex Fourier series. Math Comput 19:297

De Gennes PG (1979) Scaling concepts in polymer physics. Cornell University Press, Ithaca

Doi M (1996) Introduction to polymer physics. Oxford University Press, Oxford

Ernst RR, Anderson WA (1966) Application of Fourier transform spectroscopy to magnetic resonance. Rev Sci Instrum 37:93–102

Ferry JD (1980) Viscoelastic properties of polymers. Wiley, London

Gamota DR, Wineman AS, Filisko FE (1993) Fourier transform analysis: nonlinear dynamic response of an electrorheological material. J Rheol 37:919–933

Giacomin AJ, Dealy JM (1993) Large-amplitude oscillatory shear. In: Collyer AA (ed) Techniques in rheological measurements. Chapman and Hall, London, pp 99–121

Higgins RJ (1976) Fast FT (FFT): introduction & minicomputer experiments. Am J Phys 44:766

Holly EE, Venkataraman SK, Chambon F, Winter HH (1988) Fourier transform mechanical spectroscopy of viscoelastic materials with transient structure. J Non-Newtonian Fluid Mech 27:17–26

Homans SW (1989) A dictionary of concepts in NMR. Clarendon Press, Oxford

Larson RG (1988) Constitutive equations for polymer melts and solutions. Butterworths, London

Macosko CW (1994) Rheology principles, measurements, and applications. VCH, Wiley, New york

Malkin AY (1995) Non-linearity in rheology – an essay of classification. Rheol Acta 34:27–39

Öttinger HC, Zylka W (1992) On the relaxation spectra for models of dilute polymer solutions. J Rheol 36:885–910

Ramirez RW (1985) The FFT fundamentals and concepts. Prentice-Hall, Engelwood Cliffs

Rouault Y, Kremer K (1999) Harmonics in the rheological stress response of polymers (to be published)

Reimers MJ, Dealy JM (1996) Sliding plate rheometer studies of concentrated polystyrene solutions: large amplitude oscillatory shear of very high molecular weight polymer in dieethylphthalate. J Rheol 40:167–186

Reimers MJ, Dealy JM (1998) Sliding plate rheometer studies of concentrated polystyrene solutions: Nonlinear viscoelasticity and wall slip of two high molecular weight polymers in tricresyl phosphate. J Rheol 42:527–548

Reinheimer P, Wilhelm M, Ortseifer M, Spiess HW (1999) (to be published)

Schmidt-Rohr K, Spiess HW (1994) Multidimensional solid-state NMR and polymers. Academic Press, London

Skoog DA, Leary JJ (1992) Principles of instrumental analysis. Saunders College Publishing, Fort Worth

Wilhelm M, Maring D, Spiess HW (1998) Fourier-transform rheology. Rheol Acta 37:399–405